Investigating Crystal Structures using X-Ray Diffraction: A study of LiF and RbCl

Gwen Liu and Isabelle Boegholm
Advanced Laboratory, Physics Department,
College of Arts and Sciences,
Boston University, Boston, MA 02215, USA

(Dated: November 13, 2023)

Crystallography involves the study of the structure of materials and solids. By collecting and analyzing the X-ray diffraction spectrum of two crystals: lithium gluoride (LiF) and rubidium chloride (RbCl), we calculated the distances between the atoms in each compound, which form a cubic lattice. For LiF we measured a lattice constant of 393 pm ± 8 pm, for RbCl we measured a lattice constant of 317 pm ± 5 pm.

I. INTRODUCTION

X-ray crystallography is a foundational tool in materials science, playing a critical role in determining the atomic and molecular structures of diverse crystalline substances. Crystallography was pioneered by Lawrence Bragg and William Henry Bragg in 1912 when they found that X-ray spectrometry could provide insights to positions of atoms in a crystal [1]. This method utilizes X-rays to probe the diffraction patterns generated by the lattice spacings, which act as gratings. The resulting characteristic spectrum provides valuable insights into the material's composition and structural arrangement.

We investigated the crystal structures of lithium fluoride (LiF) and rubidium chloride (RbCl) by collection and analysing X-ray diffraction patterns. These spectrums were achieved by directing a beam of X-rays onto the surface of each crystal, and measuring the intensity of the diffracted X-ray at each incident angle.

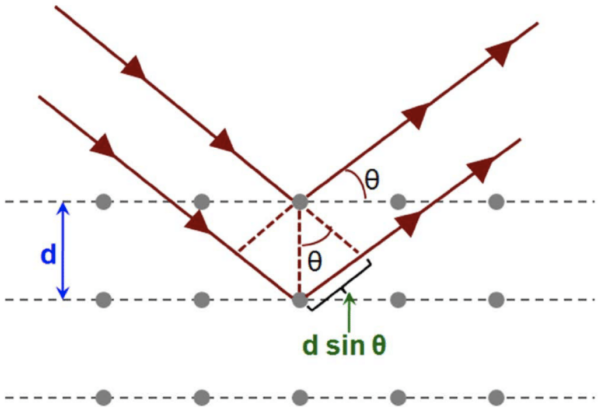

FIG. 1. An illustration of the reflection of incident X-rays according to Bragg's law and the lattice structure of a crystal

II. THEORY

X-rays are high energy electromagnetic waves, which means they have shorter wavelengths ranging from 10 picometers to 10 nanometers. X-rays are produced when a beam of high-energy charged particles, typically electrons, collide with matter. With the 580 Tel-X-Ometer apparatus, the process involves heating a filament to emit electrons, which are then accelerated within a vacuum by a strong electric field ranging from 20 to 60 kV towards a positively charged copper target, thus generating X-rays.

X-rays incident on a crystal scatter off of the atoms of the lattice, experiencing constructive interference at specific angles, dependent on the crystal's structure and the wavelength of the X-rays. Conversely, if the incident X-rays do not meet the criteria for constructive interference, destructive interference occurs. This results in a diffraction pattern and higher counts of the number of X-ray counts detected at angles where constructive interference occurs. The inter-atomic of lattice spacing, d, of the crystal is determined by Bragg's Law:

$$2d\sin(\theta) = n\lambda. \tag{1}$$

where n is a positive integer, λ refers to the wavelength of the incident X-ray, and θ represents the incident angle. [2]

Different types of X-rays are generated during this process, including characteristic X-rays resulting from the excitation of copper atoms. Specifically, when incoming electrons possess the correct energy to excite copper atoms, characteristic X-rays are emitted. In this process, electrons residing in the K shell (the innermost shell) are excited to the outer shells (L or M), creating a vacancy in the K-shell. An electron from a higher shell (L or M) subsequently drops down to the K shell to fill the vacancy, and the emitted X-rays exhibit a characteristic wavelength corresponding to the energy difference between these shells. [2]

In our experimental setup, we observe two types of characteristic X-rays: K_α and K_β, corresponding to the L and M shells, respectively. Additionally, other types of X-rays can be emitted, such as those resulting from

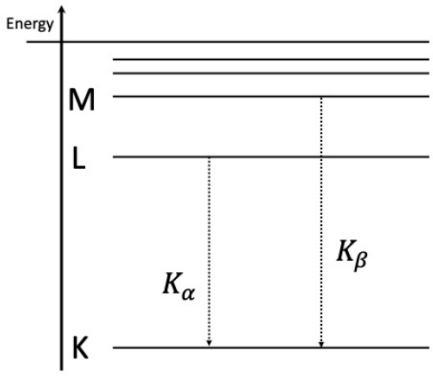

FIG. 2. K_α and K_β characteristic X-rays of Cu atoms are emitteed by electron transitions from the M or L shells to the innermost K shell.

bremsstrahlung, where X-rays are generated due to the deceleration of electrons, however their intensities are much lower than those of K_α and K_β.

These principles provide the foundation for our investigation into X-ray diffraction and emission, allowing us to gain valuable insights into the atomic arrangement and dynamics of the materials under study. The crystals we studied, lithium fluoride (Lif) and rubidium chloride (RbCl), only have one lattice constant a due to their cubic structure. We combined Bragg's law with an the relation between the lattice constant and the interatomic spacing d:

$$a = 2d. \tag{2}$$

which results in an equation for the lattice constant:

$$a = \frac{n\lambda}{\sin(\theta)}. \tag{3}$$

where θ refers to the incident angle, and λ the wavelengths of characteristic X-rays.

III. APPARATUS

The study was made using a 580 Tel-X-Ometer, a spectrometer that detects the absorption and reflection of x-rays. The Tel-X-Ometer generates X-rays in a hard vacuum, hot cathode tube with a copper target anode. The X-ray tube protrudes through the cast aluminum base of the spectrometer table, encased in a lead-glass transparent dome. The device has a sample holder at the center to mount a crystal in the path of X-rays to reflect for detection.

A Geiger counter is mounted on the end of a carriage arm and detects the the number of X-ray counts. It is connected to a Nucleus Model 500 scaler which records detection counts for .5, 1, 2, and 5 minute intervals. The scaler can be adjusted to regulated output voltages between 0 and 2 kV. The carriage arm is a movable structure that pivots around the center to adjust the angle of measure from the incident beam on the target crystal. The minimum setting is at 12 degrees to a maximum of 124 degrees. The aluminum base is labeled to a 1 degree precision, measuring the 2θ of the reflection, with a thumb-wheel that offers a 10' precision. The carriage arm assembly also has slots with numbered positions that allows for collimator slides to be positioned in front of the Geiger counter. [3]

A multimeter is connected to the X-ray tube current to monitor the current range between 40 and 80 microamps.

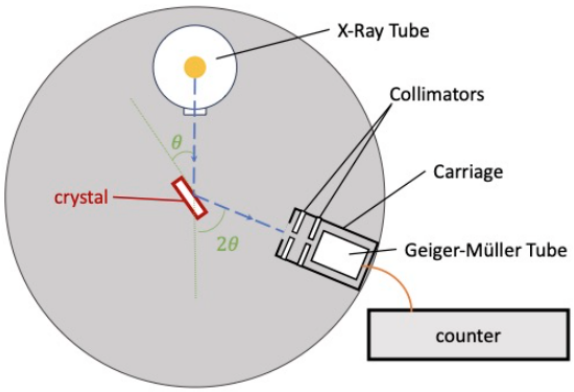

FIG. 3. Positioning of the X-ray tube, crystal, and detector in the Tel-X-Ometer setup.

IV. EXPERIMENTAL PROCEDURE

The initial crystal chosen for this experiment was lithium fluoride (LiF). The LiF crystal was oriented vertically and placed within the Tel-X-Ometer apparatus with its smooth side positioned facing the X-Ray tube. This orientation ensured that the smooth side would serve as the reflecting surface for the incident X-rays. Additionally, two collimators, one each of 3 mm aperture, were positioned in the slots numbered 25 and 30 in front of the Geiger-Muller counter, enhancing the precision measuring X-ray intensities corresponding to angles.

Prior to data acquisition, the Tel-X-Ometer was powered on and allowed to stabilize for a few minutes to ensure optimal functioning. Data acquisition commenced by capturing counts at 30-second intervals over a range of 20 degrees to 100 degrees in the double angle (2θ), with a one-degree increments for each trial. Noteworthy 2θ regions displaying spikes in the count rate were investigated further by collecting data at smaller increments of 0.5 degrees to achieve higher resolution.

Following the analysis of LiF, the experiment proceeded to investigate a second crystal, rubidium chloride (RbCl). The same protocol as for LiF was employed for data collection on the RbCl crystal. However, due to the fluctuations in measurements from noise which resulted in unclear peaks, a modification was made to the collimator setup. Specifically, one of the two 3 mm collimators was exchanged for a 1 mm collimator, with the 1 mm collimator positioned closest at slot 25 to the Geiger-Muller counter. This adjustment was intended to reduce noise and aid in obtaining higher specificity in angles for peaks.

To ascertain the background noise associated with the experimental setup, data was gathered without placing any crystal in the Tel-X-Ometer. The data was collected over the same 20 degrees to 100 degrees range, incrementing by 5 degrees.

In order to quantify the error in the measured count rate, multiple measurements were taken at the same angle corresponding to a peak. This approach allowed for a comprehensive assessment of count rate variations and provided insights into the experimental precision at specific 2θ values.

V. DATA ANALYSIS

We plot the count rates as a function of the incident angle 2θ for Lif and RbCl, seen in Figure 4. Peaks were identified by analyzing points where there were notable spikes in the count rate. Each peak was then fitted with a Gaussian curve, allowing for accurate determination of the peak positions.

The Gaussian fit provided a well-fitted curve for each peak, with the center of the Gaussian curve representing the peak position in terms of 2θ. The standard deviation (σ) of the Gaussian curve provided information about the width of the peak, reflecting the resolution of angle for that particular reflection. The wavelengths of the characteristic X-rays are:

$K_\alpha = 154$ pm $\pm$ 1 pm

$K_\beta = 138$ pm $\pm$ 1 pm

The most recent published measurements of lattice constants for LiF and RbCl are:

LiF: a = 402 pm [4]

RbCl: a = 327 pm [5]

We calculated the lattice constant from the 2θ values obtained from the Gaussian fits using Equation 3.

	n	K	2θ	a (pm)	deviation (%)
LiF	1	K_α	41.9 $\pm$ 1.17	386 $\pm$ 10	4.0
LiF	1	K_β	48.4 $\pm$ 2.65	391 $\pm$ 8	2.7
LiF	2	K_α	88.4 $\pm$ 0.99	396 $\pm$ 10	1.5
LiF	2	K_β	101.2 $\pm$ 1.25	399 $\pm$ 4	0.7
RbCl	1	K_α	57.9 $\pm$ 0.56	318 $\pm$ 3	2.8
RbCl	2	K_β	52.3 $\pm$ 1.03	315 $\pm$ 6	3.7

By taking the average we calculated our final lattice constants

LiF: a = 393 pm $\pm$8pm (2.2%)

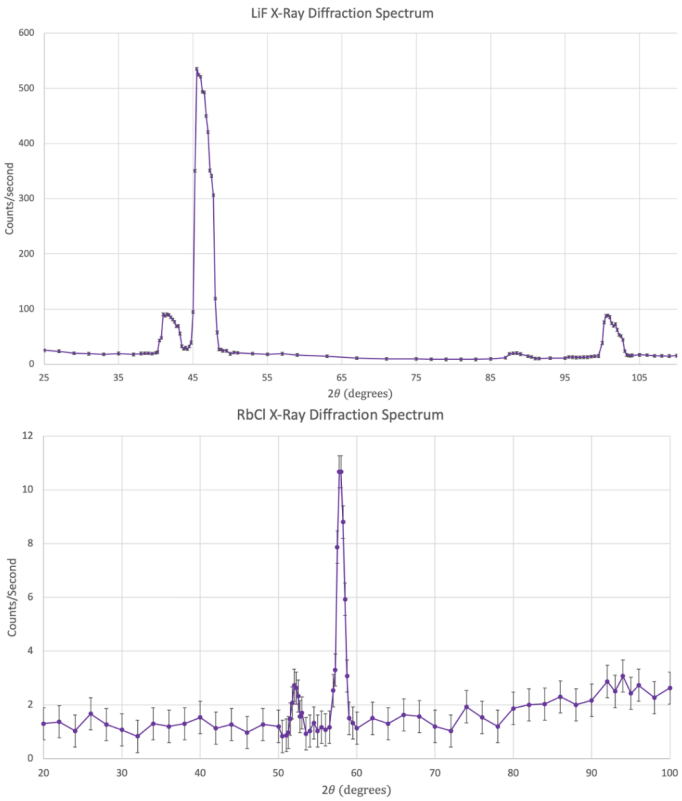

FIG. 4. X-ray diffraction spectrum for Lif and RbCl: count rates are plotted as a function of 2θ. In the LiF X-Ray spectrum, the first peak corresponds to $n = 1$ and K_β X-rays, followed by the $n = 1$ and K_α peak, the $n = 2$ and K_α peak, the $n = 2$ and K_α peak. In the RbCl spectrum, the first peak corresponds to $n = 1$ and K_β X-rays, the second to the $n = 1$ and K_α.

RbCl: a = 317 pm $\pm$ 5 pm (3.1%)

Sources of error result from the precision of the determining the angle 2θ and the fluctuations that contributed to the count rates. The measurement of angles could be made to a precision of approximately $\frac{1}{12}$ of a degree. Even with this precision and additional beam collimators to narrow the angles of peak intensities of X-ray count rates, the width of Gaussian fits demonstrate a width of uncertainty for peak angles. On average, the standard deviation was 1.28 degrees, which corresponds to approximately a range of $\pm$5 pm, or a deviation of 3% from recently published results.

The count rates observed exhibited fluctuations of 2.5 counts per second at the peaks for the LiF crystal, and 0.7 counts per second at intensity peaks for RbCl. We also monitored the currented, which fluctuated between 60 to 80 microamps. Variations in current could affect the X-ray intensity and thus the count rates. Fluctuating counts affect the precision of locating peak angles, introducing uncertainty. This was a more pronounced problem in obtaining the spectrum for RbCl where count fluctuations obscured the peaks for n=2 that we expected

to see at higher 2θ values, seen in Figure 4.

VI. CONCLUSION

In this experiment, we conducted X-ray diffraction analysis on two distinct crystals: lithium fluoride (LiF) and rubidium chloride (RbCl). Through data collection and analysis, we determined the lattice constants for each crystal.

For lithium fluoride (LiF), the measured lattice constant was $393\,\mathrm{pm} \pm 8\,\mathrm{pm}$, while for rubidium chloride (RbCl), the measured lattice constant was $317\,\mathrm{pm} \pm 5\,\mathrm{pm}$.

The obtained results align with published results in recent journals. The precision in the measured lattice constants, indicated by the small standard deviations, underscores the reliability of the X-ray diffraction method for probing crystal structures.

VII. ACKNOWLEDGEMENTS

We wish to acknowledge the support of Yaokan Situ, Lawrence R. Sulak, Jacob Willig-Onwuachi, and Japnidh Thakral for offering suggestions, encouragement, and guidance.

[1] The Editors of Encyclopaedia Britannica, Bragg law, `https://www.britannica.com/science/Bragg-law`, accessed 10 October 2023.

[2] R. W. James, *The Optical Principles of The Diffraction of X-Rays* (G. Bell and Sons Ltd., 1962).

[3] *The Tel-X-Ometer, Tel. 580*, Tetron Limited, 98 Victoria Road, London NW10, England (1974).

[4] J. Thewlis, Unit-cell dimensions of lithium fluoride made from li6 and li7, Acta Crystallographica **8**, 36 (1955).

[5] G. Raunio and S. Rolandson, Lattice dynamics of nacl, kcl, rbcl, and rbf, Phys. Rev. B **2**, 2098 (1970).